Dilated Virchow-Robin spaces are a marker for arterial disease in multiple sclerosis

Benjamin V. Ineichen,[a,b,c,d,h,i,*] Carmen Cananau,[a,b] Michael Plattén,[a,b] Russell Ouellette,[a,b] Thomas Moridi,[a,e] Katrin B. M. Frauenknecht,[f,g] Serhat V. Okar,[i] Zsolt Kulcsar,[c] Ingrid Kockum,[a,h] Fredrik Piehl,[a,e] Daniel S. Reich,[i,j] and Tobias Granberg[a,b,j]

[a]Department of Clinical Neuroscience, Karolinska Institutet, Stockholm, Sweden
[b]Department of Neuroradiology, Karolinska University Hospital, Stockholm, Sweden
[c]Department of Neuroradiology, Clinical Neuroscience Center, University Hospital Zurich, University of Zurich, Zurich, Switzerland
[d]Center for Reproducible Science, University of Zurich, Zurich, Switzerland
[e]Center of Neurology, Academic Specialist Center, Stockholm Health Services, Stockholm, Sweden
[f]National Centre for Pathology (NCP), Laboratoire National de Santé, Dudelange, Luxembourg
[g]Luxembourg Centre for Neuropathology (LCNP), Laboratoire National de Santé, Dudelange, Luxembourg
[h]Center for Molecular Medicine, Karolinska Institutet, Stockholm, Sweden
[i]Translational Neuroradiology Section, National Institute of Neurological Disorders and Stroke (NINDS), National Institute of Health (NIH), Bethesda, MA, USA

Summary

Background Virchow-Robin spaces (VRS) have been associated with neurodegeneration and neuroinflammation. However, it remains uncertain to what degree non-dilated or dilated VRS reflect specific features of neuroinflammatory pathology. Thus, we aimed at investigating the clinical relevance of VRS as imaging biomarker in multiple sclerosis (MS) and to correlate VRS to their histopathologic signature.

Methods In a cohort study comprising 142 MS patients and 30 control subjects, we assessed the association of non-dilated and dilated VRS to clinical and magnetic resonance imaging (MRI) outcomes. Findings were corroborated in a validation cohort comprising 63 MS patients. Brain blocks from 6 MS patients and 3 non-MS controls were histopathologically processed to correlate VRS to their tissue substrate.

Findings In our actively treated clinical cohort, the count of dilated centrum semiovale VRS was associated with increased T1 and T2 lesion volumes. There was no systematic spatial colocalization of dilated VRS with MS lesions. At tissue level, VRS mostly corresponded to arteries and were not associated with MS pathological hallmarks. Interestingly, in our *ex vivo* cohort comprising mostly progressive MS patients, dilated VRS in MS were associated with signs of small vessel disease.

Interpretation Contrary to prior beliefs, these observations suggest that VRS in MS do not associate with an accumulation of immune cells. But instead, these findings indicate vascular pathology as a driver and/or consequence of neuroinflammatory pathology for this imaging feature.

Funding NIH, Swedish Society for Medical Research, Swiss National Science Foundation and University of Zurich.

Keywords: Multiple sclerosis (MS); Perivascular spaces; Virchow-Robin spaces; Magnetic resonance imaging (MRI); Clinical study

*Corresponding author. National Institutes of Health (NIH), National Institute of Neurological Diseases and Stroke (NINDS), Bethesda, MA, USA.
   E-mail address: Benjaminvictor.ineichen@uzh.ch (B.V. Ineichen).
[j]Authors share senior authorship.

Research in context

Evidence before this study
Perivascular spaces surround blood vessels in the brain and can become visible on MRI as Virchow-Robin spaces (VRS) when they enlarge. A solid evidence base indicates the association of VRS with ageing, vascular risk factors, vascular diseases such as small vessel disease or stroke as well as neurodegenerative disorders. VRS have also been associated with neuroinflammatory diseases such as multiple sclerosis (MS). Particularly, it has been hypothesized that VRS reflect a local accumulation of immune cells prior to a neuroinflammatory attack. This study aimed to investigate the association of nondilated and dilated VRS with clinical and imaging parameters in MS patients and to assess the histopathological signature of VRS in post-mortem brain tissue.

Added value of this study
Challenging prior beliefs, our study suggests that VRS in MS do not associate with an accumulation of immune cells. Instead, findings from our study allude toward vascular pathology as a driver and/or consequence of neuroinflammatory pathology for VRS in MS.

Implications of all the available evidence
Although the exact pathomechanisms of VRS are elusive, VRS seem to be involved in MS pathology. They could potentially be exploited as imaging biomarker, for example to enable non-invasive insights into vascular pathology in MS patients.

Introduction

Perivascular spaces surround blood vessels in the brain[1]. Macroscopically visible perivascular spaces, also referred to as Virchow-Robin spaces (VRS) or enlarged perivascular spaces, are readily detectable by magnetic resonance imaging (MRI).[2,3] VRS appear as thin linear or small punctate structures with a signal similar to CSF on MRI.[4] Normally, VRS are smaller than 2 mm in diameter; yet, due to unknown reasons, VRS may dilate and present with diameters ≥2 mm.[5]

Although there is an ongoing debate about the clinical relevance of VRS,[6,7] a large body of evidence indicates their association with ageing, vascular risk factors like hypertension,[8] vascular diseases such as small vessel disease[9] or stroke[10,11] as well as neurodegenerative diseases.[12]

Accumulating evidence also suggests an association of VRS with neuroinflammatory disorders, including multiple sclerosis (MS).[3] MRI studies have shown that MS patients harbour a higher VRS burden compared to control subjects.[13,14] This has been confirmed in a recent meta-analysis.[15] Furthermore, albeit not reproduced so far, increase of overall VRS volume may precede the emergence of contrast-enhancing MS lesions.[16] Finally, it has been shown that MS patients have elevated numbers of dilated VRS.[17]

Together, the exact roles of both nondilated and dilated VRS in MS pathogenesis are insufficiently understood. To further corroborate nondilated and/or dilated VRS as an imaging biomarker in MS, several open questions need to be answered: (1) Are VRS cross-sectionally or longitudinally associated with clinical or imaging outcomes in MS? (2) What is the topographical distribution of VRS, and do they coincide with MS lesions? (3) What is the longitudinal evolution of VRS in MS? And (4) What is the anatomical and/or pathological substrate of VRS in MS, and could they also be associated with signs of vascular diseases in MS?

Here, we studied nondilated and dilated VRS in the largest MS patient cohort to date, collectively comprising 205 patients (including 24 patients with longitudinal MRI scans) and 30 controls, with prospective collection of clinical outcomes and standardized T1- and T2-weighted (T1w, T2w) MRI. Finally, in brain samples from MS donors and non-MS controls with corresponding pre- and post-mortem MRI scans, we assessed the anatomical and pathological signature of VRS on the tissue level.

Methods

Study design and subjects

Our exploratory cohort comprised 142 MS patients and was derived from the *Stockholm Prospective Assessment of MS* (STOP-MS, an incidence cohort) from the Karolinska University Hospital in Sweden (including 24 patients with longitudinal data). The validation cohort constitutes a subcohort of the *MultipleMS* (incidence cohort comprising subjects with newly diagnosed CIS/MS between 18 and 50 years old) and *MyelinMS* (MS subjects with available CSF sample) studies conducted at the same institution and comprised 63 MS patients. The control cohort consisted of 30 sex- and age-matched subjects imaged on the same scanner. All studies include longitudinal follow-up including standardized MRI scanning protocols at 3 T and longitudinal clinical evaluations. Inclusion criteria for our study: subjects with T1w and T2w as well as T2w-fluid-attenuated inversion recovery (FLAIR) MRI. In addition, for the histopathologic assessment, brains from 9 subjects were included (6 MS patients, 3 non-MS patients). Patients with a history of stroke or cardial infarction were excluded.

Clinical outcomes

Clinical disability of the patients was assessed using the Expanded Disability Status Scale (EDSS).[18] Cognitive functioning was measured by the Symbol Digit Modalities Test (SDMT).[19] The cognitive scores were normalized to age- and sex-adjusted *z*-scores based on

normative data.[20] For the STOP-MS cohort, vascular risk profiles were compiled based on the presence of diabetes, dyslipidemia, hypertension, smoking status, and antiplatelet therapy.

In vivo MRI

Imaging was performed on the same Siemens Trio/PRISMA[Fit] 3 T MRI scanner (Siemens Healthcare, Erlangen, Germany) with a 20-channel head coil. The protocol included: (1) A 3D T1w sequence (repetition time = 1900 ms, echo time = 3.39 ms, inversion time = 900 ms, flip angle = 9°, spatial resolution $1.0 \times 1.0 \times 1.5$ mm^3), for VRS detection, atrophy measurements, and T1 lesion detection; (2) The same 3D T1w sequence was applied after intravenous administration of a standard dose (0.2 ml/kg) of gadoteric acid (Dotarem) after a minimum of 5 min delay, which was administered as part of the clinical routine; (3) A 3D T2w sequence (repetition time = 3200 ms, echo time = 388 ms, flip angle = 120°, spatial resolution $1.0 \times 1.0 \times 1.0$ mm^3); and (4) A 3D T2w FLAIR (TR = 6000 ms, TE = 388 ms, TI = 2100 ms, flip angle = 120°, spatial resolution $1.0 \times 1.0 \times 1.0$ mm^3) for T2 lesion detection.

Within cohorts, pre- and post-contrast T1w images, T2w, and T2w FLAIR images were registered to each other by linear/affine registration using the FSL's Linear Image Registration Tool (FLIRT).[21]

Lesion and brain atrophy measures

FreeSurfer version 6.0.0 was used to perform automated cross-sectional and longitudinal brain volume measures and segment T1 hypointense lesions.[22] For volumetric analyses, gray and white matter volume as well as whole brain volume were normalized to the estimated total intracranial volume, resulting in the corresponding tissue fractions.[23] To estimate longitudinal brain atrophy rates, the longitudinal stream of FreeSurfer was used to obtain the white matter, gray matter, and brain parenchymal fractions (WMF, GMF, and BPF). Numerically, the latest available MRI measurement was subtracted by the earliest available MRI measurement, divided by the time in between the scans. Lesion Segmentation Toolbox (LST) 2.0.15[24] for SPM12 was used to perform cross-sectional and longitudinal T2 lesion volume segmentations based on the FLAIR volumes. The volumes of contrast-enhancing lesions were manually segmented on the post-contrast 3D T1-weighted images using ITK-SNAP.[25]

Assessment of VRS

VRS were defined according to the STRIVE criteria, i.e., as fluid-filled spaces that follow the typical course of a vessel through gray or white matter and with similar signal intensity to CSF on all sequences.[1] VRS were quantified on the axial and coronal reformatted T1-weighted images by a resident in neuroradiology (BVI) with 2 years of training using the open source DICOM viewer Horos (blinded to the MS or control status). T2w-FLAIR images were consulted to differentiate VRS from MS lesions (hyperintense on T2 FLAIR) or lacunar infarcts (commonly with hyperintense rim). Following prior work,[13] four brain levels were used as landmarks to assess VRS: (1) the hand knob at the high convexity/centrum semiovale, (2) at the widest part of the crus anterius, (3) at the level of the anterior commissure and (4) in the midbrain at the largest interpeduncular distance (Fig. 1a–e). We decided post-hoc to pool VRS at the two levels of the basal ganglia by using their mean to reduce the number of statistical tests. Additionally, VRS outcomes were rated by an experienced neuroradiologist (CC) on 25 randomly selected MRI scans to estimate the inter-rater agreement.

The following predefined VRS characteristics were assessed: (1) Total VRS counts were quantified for each of above-mentioned brain levels. (2) VRS counts with a diameter of ≥2 mm (hereafter referred to as "dilated VRS" Fig. 1f) were quantified on coronally reformatted T1 slices by measuring the widest diameter. The cutoff of 2 mm was based on previous studies assessing VRS.[5,17,26] (3) VRS volumes were determined by manually segmenting VRS on FLAIR-registered, coronally reformatted T1-weighted images using Freeview and FMRIB Software Library (FSL) UTILS.[21]

To investigate spatial association of VRS to MS lesions, for each subject, binary VRS and lesion masks were created. The FreeSurfer segmentation output and the LST output were used as templates for T1 and T2 lesion masks, respectively. These templates, as well as the manually segmented VRS masks, were resampled to their original T1w image using FSL's FLIRT and subsequently binarized using FSL UTILS.[21] For visualization, the VRS masks were resampled and superimposed to the average space MRI of the respective cohort generated using fsaverage from FreeSurfer, registered by FSL's FLIRT. In order to quantify the lesion volume in proximity to VRS, VRS masks were expanded by two voxels on each axis using FSL UTILS and the overlap between lesions and expanded VRS masks was assessed. We hypothesized that dilated VRS have a larger overlap with MS lesions compared to non-dilated VRS.

Postmortem MRI

Postmortem MRI scans from MS brains were acquired as previously described.[27] Briefly, formalin-fixed brains were positioned in a Fomblin-filled container and were scanned in a 7-T MRI scanner (Siemens) equipped with a birdcage-type transmit coil and a 32-channel receive coil. A 3D T1w magnetization-prepared rapid gradient echo (T1-MP2RAGE, repetition time = 2200 ms, echo time = 3.04 ms, flip angle = 7°, nominal resolution $0.6 \times 0.6 \times 0.6$ mm^3, acquisition time: 6 min, 35 s) and a 3D high-resolution multigradient-echo (GRE, repetition
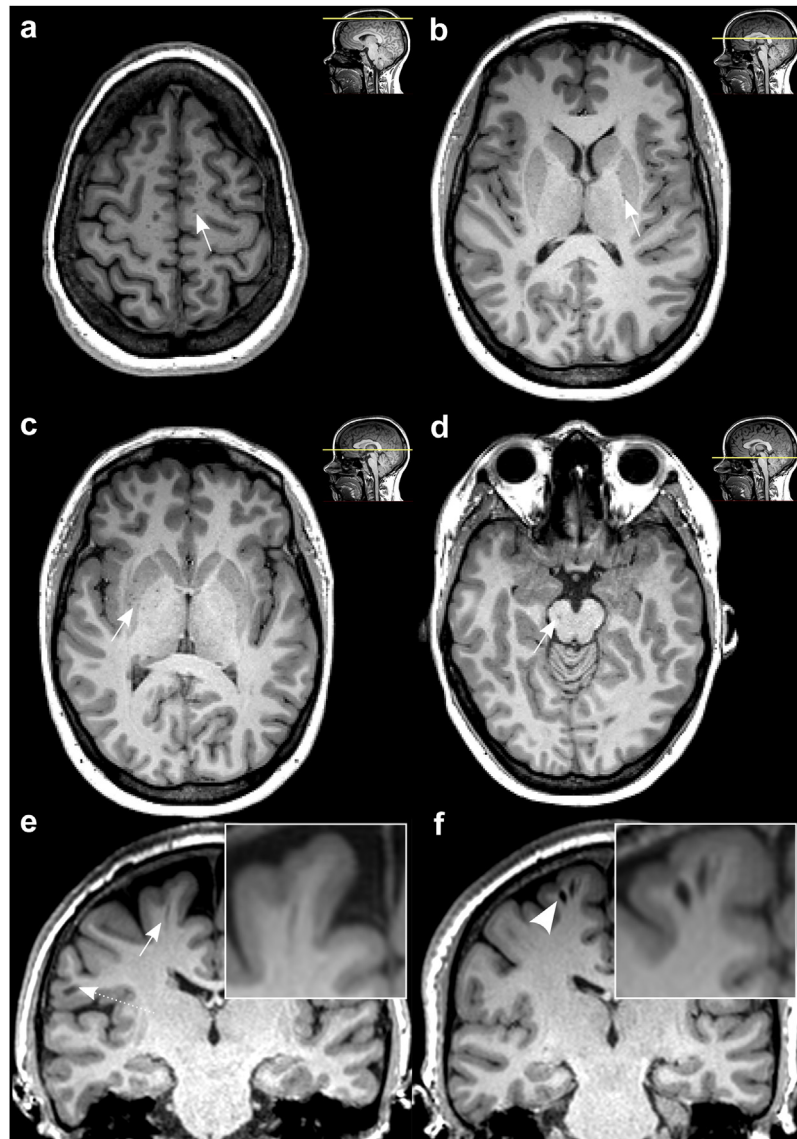
Fig. 1: Virchow-Robin spaces (VRS) are readily detectable on T1-weighted brain MRI scans. (a–d): VRS were assessed at 4 different brain levels: centrum semiovale (a), basal ganglia, crus anterius and anterior commissure (b and c), and brain stem (d).[13] Arrows indicate VRS on an axially reformatted MRI slices. (e and f): Coronally reformatted MRI slice with one nondilated VRS ((e), arrow, diameter < 2 mm, dashed arrow indicates a juxtacortical MS lesion) and two dilated VRS ((f), arrowhead, diameter ≥ 2 mm) from two different MS patients, both with relapsing MS phenotype. *Abbreviations: MS, multiple sclerosis; MRI, magnetic resonance imaging; VRS, Virchow-Robin spaces.*

time = 60 ms, echo times = 6.09, 15.99, 25.89, and 35.79 ms, flip angle = 10°, nominal resolution $0.42 \times 0.42 \times 0.42$ mm^3, acquisition time: 2 h, 15 min) T2*w sequence were acquired. Pre- and post-mortem MRI scans were registered by linear/affine registration using an in-house software.

Histopathology
Histopathological validation of MRI findings was performed as described previously.[28] Briefly, brains were placed in individualized cutting-boxes and were sectioned to 1-cm-thick coronal slices. The match between the gross anatomy of the slices and the coronal T1w data was determined visually according to cortical and ventricular profiles. From these samples, VRS-corresponding tissue features were identified. We selected VRS based on their distinct macroscopic appearance on the brain slab and their correspondence to either pre- or postmortem MRI. Subsequently, these brain regions were sliced to 5-μm-thick sections using a

microtome. Slides were stained with hematoxylin and eosin (H&E), Luxol fast blue-periodic acid Schiff (LFB-PAS), and, to assess vascular pathology, with Verhoeff van Gieson as well as congo red.[29] Additionally, a panel of different immunohistochemistry stains was applied to evaluate anatomy and pathology of the perivascular spaces and the adjacent CNS parenchyma, including CD3, Iba1, PLP, NFL, fibrinogen, laminin a1, collagen IV a1, and aquaporin-4 (AQP-4) (Supplementary Table S1).

Two raters (KBMF, a board-certified neuropathologist, and BVI) independently assessed pathological VRS features in a blinded fashion. Blood vessels were identified as veins or arteries based on Verhoeff van Gieson staining. CD3, PLP, and neurofilament light chain immune stainings were used to assess immune cellularity, (de)myelination status, and axonal damage adjacent to dilated and nondilated VRS, respectively. All stainings were semiquantitatively evaluated to assess respective pathology (score from 0 to 4 for each outcome). Additionally, vascular disease was semiquantitatively assessed by the presence of endothelial proliferation, splitting of the lamina elastica interna, microatheroma (i.e., presence of lymphocytic/monocytic infiltration to vessel walls), concentric hyaline thickening, perivascular hemosiderin deposition, and/or vascular tortuosity[29] (each accounting for 1 point, i.e., score of 0–6 per vessel).

Statistical analyses

Statistical analyses were performed using R statistical software version 3.5.2. We did not conduct an *a priori* sample size calculation, instead the study was based on a convenience sample. Univariate linear regression modelling was used to assess potential associations between VRS and outcome measures which were, if explicitly stated, adjusted for sex, age, and vascular risk factors. Group differences were tested using a two-tailed t-test in case of normally distributed data and a Mann–Whitney U-test in case of nonparametric data. P values < 0.05 were considered statistically significant. In order to assess the association between VRS dynamics and other imaging and clinical features, we applied two approaches: 1) assessing correlation between VRS measures and clinical outcomes and 2) stratifying patients into groups with either VRS volume increase or decrease. Multiple comparisons adjustment using a Benjamini–Hochberg correction was applied to control for false discovery rates (association of VRS to demographic parameters: 10 tests; comparison of VRS measures between MS and controls: 12 tests; association between VRS and MS lesions: 4 tests; proximity analysis: 1 test; pre-postmortem MRI and histopathology: 4 tests; longitudinal VRS analysis: 35 tests). Corrected p values are reported throughout the paper. We chose the Benjamini–Hochberg correction over procedures that control for family-wise error (such as the Bonferroni method) since it strikes a balance between controlling the false discovery rate and maintaining statistical power, thus being a suitable choice for larger-scale studies with a larger number of hypotheses.

Ethics and study approval

All clinical studies were approved by the regional ethics review boards of Stockholm (STOP-MS No. 2009/2017-31/2, last amendment 2022-01015-02; MultipleMS 2017/1323-31, amended 2018/2713-32; MyelinMS No. 2018/903-31/2), and informed consent was obtained from all participants. The formalin-fixed brains were attained at autopsy after consent was obtained from the next of kin.

Role of funders

The funders had no role in the design and conduct of the study; collection, management, analysis, and interpretation of the data; preparation, review, or approval of the manuscript; and decision to submit the manuscript for publication.

Results

Cohort demographics and participant characteristics

Three separate clinical cohorts were included in this study: (1) the exploratory MS cohort including 142 MS patients; (2) the validation MS cohort including 63 RRMS patients; and (3) an age-matched healthy control cohort including 30 individuals. There was no difference in sex or age distribution between either of the cohorts. The rationale of including two separate clinical MS cohorts, i.e., an exploratory and validation cohort, comes from an attempt to probe the robustness of our initial findings in the first (exploratory) cohort. We decided post-hoc to pool these two cohorts. Findings for the individual cohorts and for the pooled cohorts are reported separately in the manuscript.

In total, 38 of 142 subjects (27%) had at least one vascular risk factor. At time of imaging, 171 of 205 MS patients (83%) underwent disease modifying therapy (DMT; 50 interferon beta, 50 rituximab, 32 dimethyl fumarate, 25 natalizumab, 14 glatiramer acetate) and 30 patients did not receive DMT (15%). Participant demographics and disease characteristics are summarized in Table 1.

Age and sex as contributor to VRS counts and volumes in the primary cohort

There was substantial agreement in Cohen's kappa for VRS counts and volume between two raters (κ = 0.69–0.72, p < 0.001).

In the exploratory MS cohort, higher age and male sex were associated with higher centrum semiovale VRS counts (β = 0.02, p = 0.02 and β = 0.31, p = 0.04, respectively) and volumes (β = 3.69 μl, p = 0.005 and β = 66.18 μl, p = 0.02, respectively). Female sex was a significant positive contributor to basal ganglia VRS

Cohort	Control	Exploratory	Validation
Number of subjects	**30**	**142**	**63**
Sex			
Female	23 (77%)	95 (67%)	48 (76%)
Male	7 (23%)	47 (33%)	15 (24%)
MS phenotype			
Relapsing-remitting	N/A	113 (80%)	63 (100%)
Secondary-progressive	N/A	23 (16%)	0
Relapsing-progressive	N/A	2 (1%)	0
Primary-progressive	N/A	4 (3%)	0
Median age (range) [years]	**38 (18–65)**	**36 (16–66)**	**35 (18–50)**
Median EDSS (range)	**N/A**	**2.0 (0–8.0)**	**1.0 (0–4.5)**
Median disease duration (range) [years]	**N/A**	**6.3 (0–43)***	**3.4 (0–31)***
Disease-modifying therapy (DMT)			
Interferon beta (%)	N/A	33 (23%)	17 (27%)
Natalizumab (%)		17 (12%)	8 (13%)
Rituximab (%)		36 (25%)	14 (22%)
Dimethyl fumarate (%)		25 (18%)	7 (11%)
Glatiramer acetate (%)		9 (6%)	5 (8%)
Number of MRI scans			
1 scan	30 subjects	142 patients	63 patients
2 scans	0	20 patients	0
3 scans	0	4 patients	0
Median follow-up (range) [months]	**N/A**	**18 (4–48)**	**N/A**
Disease characteristics			
Median T1 lesion volume (range) [ml]	N/A	1.7 (0.7–32)	0.3 (0.4–7.2)
Median T2 lesion volume (range) [ml]	N/A	2.6 (0.1–125))	1.3 (0–66.2)
Median BPF (range) [%]	77 (65–80)	72 (64–85)	74 (69–87)
Vascular risk factors			
Diabetes	N/A	9 (6%)	N/A
Hypertension	N/A	21 (15%)	N/A
Dyslipidemia	N/A	11 (8%)	N/A
Antiplatelet	N/A	11 (8%)	N/A
Smoking	N/A	17 (12%)	N/A

Data shown for the two MS cohorts (exploratory and validation cohort) as well as for the control cohort. The validation cohort had a shorter disease duration compared to the exploratory cohort (p = 0.02, Mann–Whitney U test). There were no statistically significant differences between the cohorts regarding sex, MS phenotype, age, or EDSS. Median estimated disease duration is based on time since symptom onset. Asterisks indicate statistical significance between cohorts: *p < 0.05. Abbreviations: BPF, brain parenchymal fraction; EDSS, Expanded Disability Status Scale; N/A, not available.

Table 1: Participant demographics and disease characteristics at baseline.

(β = 0.28, p < 0.001). Increasing age was a significant positive contributor to basal ganglia VRS volume (β = 0.93, p = 0.01). There were no associations with age or sex for dilated VRS (i.e., VRS with a diameter ≥2 mm). These associations were not reproduced in the validation or control cohorts, hence while we adjusted for age and sex in subsequent analyses, we did not consider disease status as a modifier of these potential associations.

MS patients have greater VRS counts and volumes compared to control subjects

Median VRS counts differed significantly between MS patients and controls in the centrum semiovale (exploratory cohort: 7 [range: 0–41]; validation cohort: 10 [2–34]; pooled MS cohort: 8 [0–41] versus control: 4 [1–14], p = 0.002, p < 0.001, and p < 0.001, respectively) and basal ganglia (exploratory cohort: 6 [2–23], validation cohort: 5 [0–10]; pooled MS cohort: 6 [range 1–23] versus control: 3 [2–9], p < 0.001, p = 0.31, and p = 0.009, respectively; Table 2, Fig. 2a, and Supplementary Figure S1a). Similarly, the median VRS volume (range) in the centrum semiovale was greater in MS patients compared to controls (exploratory cohort: 249 μl [161–1141]; validation cohort: 253 μl [22–900]; pooled MS cohort: 250 μl [22–1141] versus control: 90 μl [8–588], p < 0.001, p = 0.03, and p = 0.002, respectively; Table 2, Fig. 2b, and Supplementary Figure S1b). Finally, the median count of dilated VRS was greater in MS patients compared to controls (exploratory cohort:

Cohort	Control	Exploratory	Validation	Pooled MS
Number of subjects	30	142	63	205
Prevalence of VRS per location (%)				
Centrum semiovale	30/30 (100%)	137/142 (96%)	63/63 (100%)	200/205 (98%)
Basal ganglia	30/30 (100%)	142/142 (100%)	63/63 (100%)	205/205 (100%)
Brain stem	14/30 (47%)	44/142 (31%)	15/63 (24%)	59/205 (29%)
Median VRS count per location (range)				
Centrum semiovale	4 (1–14)	**7 (0–41)****	**10 (2–34)*****	**8 (0–41)*****
Basal ganglia	3 (2–9)	**6 (2–23)*****	5 (0–10)	**6 (1–23)****
Brain stem	0 (0–1)	0 (0–1)	0 (0–1)	0 (0–1)
Median VRS volume per location [µl] (range)				
Centrum semiovale	90 (8–588)	**249 (161–1141)*****	**253 (22–900)***	**250 (22–900)****
Basal ganglia	176 (0–491)	143 (68–395)	151 (18–271)	146 (18–395)
Brain stem	N/A	N/A	N/A	N/A
Median count of dilated VRS (diameter ≥ 2 mm, range)				
Centrum semiovale	0.20 (0–3)	**0.83 (0–9)***	**1.22 (0–7)****	**0.95 (0–9)***
No of patients with VRS ≥ 2 mm (%)	4 (13%)	**43 (30%)****	**31 (49%)****	**74 (36%)****

Higher centrum semiovale and basal ganglia VRS counts and centrum semiovale VRS volumes in MS patients compared to controls (Control cohort n = 30; exploratory cohort: n = 142; validation cohort: n = 63; pooled MS cohorts: n = 205). Asterisks indicate statistical significance between compared to the control cohort, statistically significant association are printed in bold font: *p < 0.05, **p < 0.01, ***p < 0.001. Abbreviations: N/A, not available; MS, multiple sclerosis.

Table 2: Virchow-Robin space (VRS) prevalence, counts, and volumes per location for the MS cohorts.

0.83 [range: 0–9]; validation cohort: 1.22 [0–7]; pooled MS cohort: 0.95 [0–9] versus control: 0.20 [0–3], p = 0.04, p = 0.002, and p = 0.01, respectively, Table 2, Fig. 2c, and Supplementary Figure S1c).

The number of dilated VRS is associated with T1 and T2 lesion volumes

VRS counts and volumes were not associated with T1 or T2 lesion volume. Interestingly, however, the number of dilated VRS (diameter ≥2 mm) in the centrum semiovale was associated with both T1 and T2 lesion volumes (β = 0.53, p < 0.001 and β = 0.93 ml, p = 0.01, respectively). These findings remained statistically significant in multivariable analysis with age, sex, supratentorial brain volume, and number of vascular risk factors as independent variables (T1 lesions: β = 0.53, p = 0.001 and T2 lesions: β = 0.93, p = 0.01; Fig. 2d and e). Additionally, findings were corroborated in the validation cohort, in which we also found associations between the number of dilated VRS and T1 or T2 lesion volumes (β = 0.31, p = 0.02 and β = 0.32, p = 0.007, respectively; Fig. 2f and g). A similar association was found when pooling the exploratory and validation cohort (β = 0.40, p < 0.001 and β = 0.59, p < 0.001, respectively; Supplementary Figure S1d and S1e). As expected, T1 and T2 lesion volume were positively correlated to each other (r = 0.88, p < 0.001). No such association was found for basal ganglia VRS in either of the cohorts. Also, no association was found between VRS counts, volume or number of dilated VRS and volume of Gd-enhancing lesions. VRS counts, volumes, or diameters were not associated with brain parenchymal fraction in the uni- or multi-variable analysis (Supplementary Table S2).

No association of VRS with clinical parameters

We did not find an association of VRS counts, diameters, or volumes with EDSS or count of total relapses. We also did not find an association of VRS counts or volumes with cognitive performance of MS patients as assessed by SDMT. DMT and DMT status (i.e., treated or untreated) were not associated with VRS measures.

No bias of T1 or T2 lesions to dilated VRS compared to non-dilated VRS

Both dilated and non-dilated centrum semiovale VRS were mainly located at the parieto-occipital transition region and in the superior cerebral convexities (Fig. 3a–c). Basal ganglia VRS were mainly located in the dorsal aspects of the putamen and the globus pallidus (Fig. 3d–f). Control subjects had a similar dispersion of centrum semiovale and basal ganglia VRS (Supplementary Figure S2).

There was only very small overlap of VRS with MS lesions (Fig. 4 and Supplementary Figure S3). There was no statistically significant difference in proximity of either T1 or T2 lesions to dilated or non-dilated centrum semiovale VRS in the validation cohort (Wilcoxon signed-rank test, for T1 lesions p = 0.33; for T2 lesions p = 0.21, Fig. 4b).

VRS changes are not associated with clinical/imaging parameters

Our exploratory cohort included 24 patients with up to 3 longitudinal MRI scans and a cumulative follow-up time
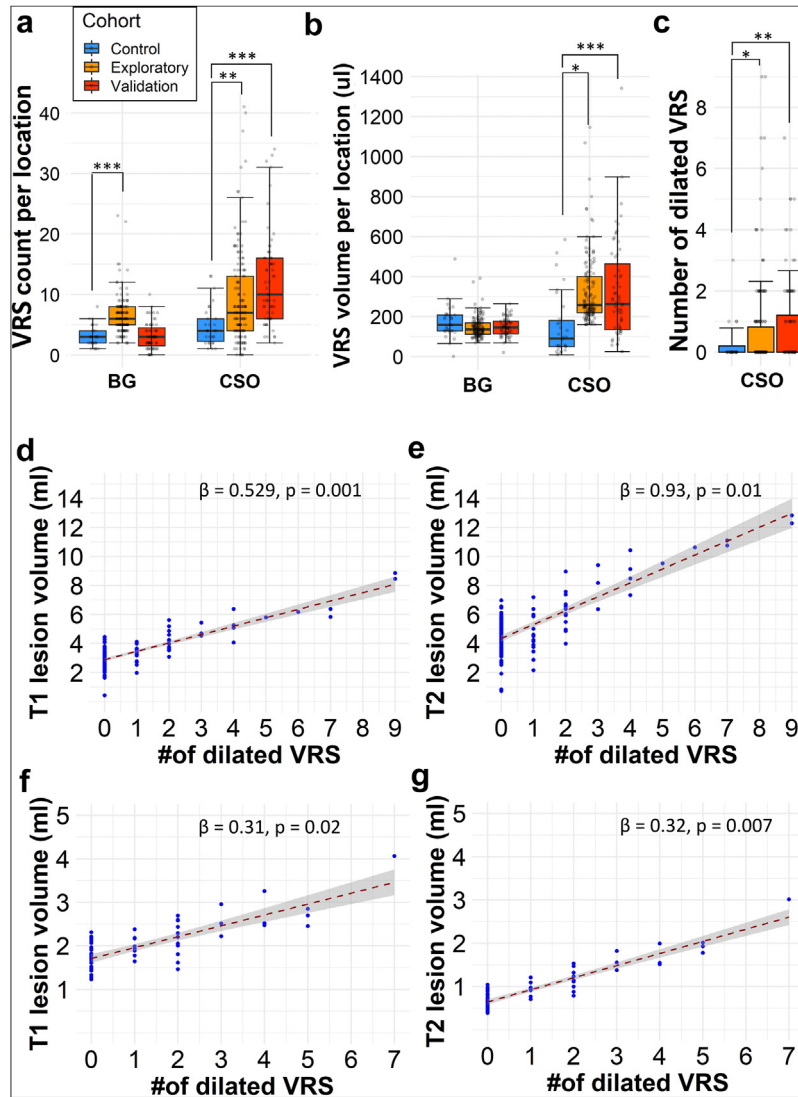
Fig. 2: Dilated VRS are associated with higher T1 and T2 lesion volumes. Higher VRS counts (a), volumes (b), and number of dilated VRS (diameter ≥2 mm, (c)) in MS patients compared to controls (Exploratory cohort: n = 142; validation cohort: n = 63; control cohort: n = 30). The count of dilated perivascular spaces (VRS, diameter ≥ 2 mm) was associated with higher MRI T1 lesion (d) and T2 lesion volume (e) in our exploratory cohort (n = 142). These associations were substantiated in the validation cohort (n = 63, (f and g)). The corresponding slope of the regression line (β) and p values are displayed at the top right corner of each graph. The regression models are adjusted for patient age and sex. Asterisks indicate statistical significance between cohorts: *p < 0.05, **p < 0.01, ***p < 0.001. *Abbreviations: BG, basal ganglia; CSO, centrum semiovale; VRS, Virchow-Robin space.*

of 31.5 patient-years (median follow-up time 18 months [range: 4–48]). MS patients showed a mostly stable disease course over the follow-up period with stable EDSS and only modestly increasing lesion volume over time (Supplementary Table S3). Three patients presented with contrast-enhancing MRI lesions during follow-up.

During the follow-up, 5 patients presented with at least 1 new T2 lesions during the follow-up and 2 patients changed DMT (from betaferon to rituximab). During the follow-up period, a total of 30 new VRS were detected, corresponding to around 1 new VRS per patient-year. Most new VRS were detected in the basal ganglia (0.51/year), followed by the centrum semiovale (0.30/year).

Overall, VRS volumes did not change significantly during the observation period in either the basal ganglia or the centrum semiovale (Supplementary Table S3). Regarding evolution of VRS diameters: 12 out of 24 longitudinally followed-up patients showed a total of 35 dilated VRS at the initial scans. Seven of these 12
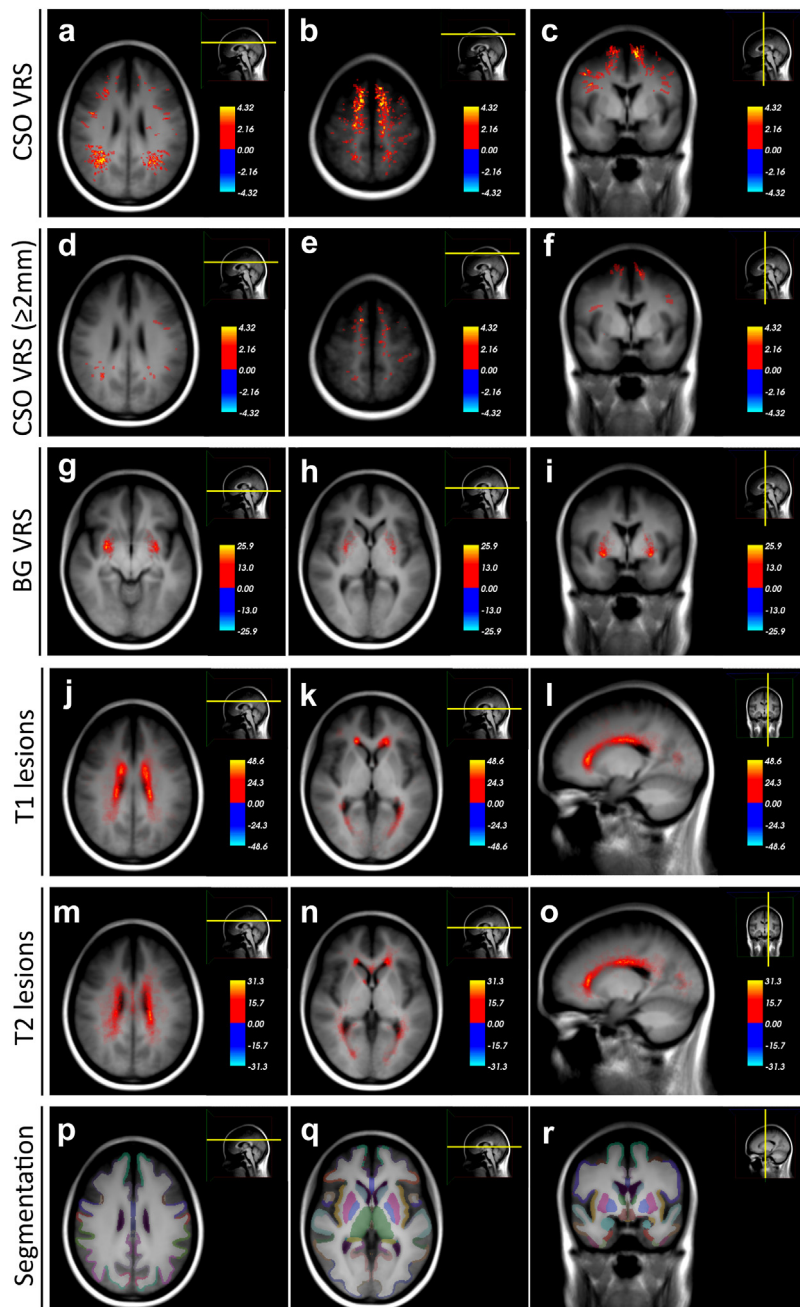
Fig. 3: VRS and MS lesion heat maps in the exploratory cohort. Heat maps of VRS and T1 lesions in the exploratory MS cohort (n = 142), superimposed on the average space MRI scan of the exploratory cohort. VRS are mainly located at the parieto-occipital transition region and in the superior convexities (a–c). Dilated VRS (diameter ≥ 2 mm) show a similar distribution (d–f). Basal ganglia VRS are mainly located in the dorsal aspects of the putamen and the globus pallidus (g–i). T1 and T2 lesions are mainly located adjacent to the lateral ventricles (j–o). For comparison, (p–r) displays the cortical and subcortical parcellation/segmentation output from FreeSurfer.[30] *Abbreviations: BG, basal ganglia; CSO, centrum semiovale; MS, multiple sclerosis, VRS; Virchow-Robin spaces.*

patients (58%) showed a total increase of 10 dilated VRS within 31.5 patient years.

In the binary analysis (i.e., stratifying the patients into VRS increase or decrease and including baseline VRS as independent variable), there was no association of VRS volume change with baseline or longitudinal imaging (gadolinium enhancing lesion volume [p = 0.32], T1 or T2 lesion volume [p = 0.44 and 0.91] as
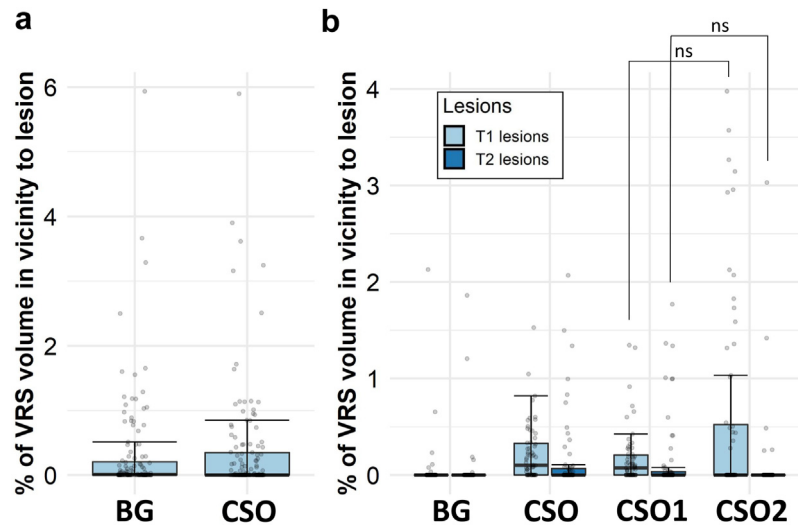
Fig. 4: Quantification of overlap between VRS and MS lesions. Percentage of volume overlap between Virchow-Robin spaces (VRS, dilated by two voxels on each side) and MS lesions in (a) the exploratory (n = 142) and (b) the validation multiple sclerosis (MS) cohort (n = 63). For the exploratory cohort, only VRS proximity to T1 lesions is displayed. Many patients show zero overlap, with some cases showing up to 6% overlap between VRS and MS lesions. There is no statistically significant difference between nondilated (CSO1) and dilated (CSO2) centrum semiovale VRS in overlap with either T1 or T2 lesions. In (b): left box/whiskers of the corresponding VRS location represents proximity to T1 lesions and right box/whiskers T2 lesions. *Abbreviations: BG, basal ganglia; SOC, centrum semiovale; VRS, Virchow-Robin spaces.*

well as brain volume [p = 0.61]) or clinical outcome measures (number of total relapses [p = 0.20], EDSS [p = 0.73], SDMT [p = 0.42]). Additionally, in a correlation analysis, there was no association between VRS changes and imaging/clinical outcomes (Supplementary Table S4). In 3 patients with contrast-enhancing MS lesions during follow-up, VRS appearance including volume remained highly stable.

Pre-post-mortem dynamics of VRS
Our post-mortem cohort comprised 6 MS patients (5 with a progressive, 1 with a relapsing clinical phenotype), 3 of them with pre-mortem MRI (Table 3). First, we assessed interrater agreement for VRS detection on post-mortem MRI: there was substantial agreement in Cohen's kappa (κ = 0.61–0.71, p < 0.001). Next, we assessed whether VRS appearance in MRI changed upon death in 3 of the patients with both pre- and post-mortem MRI. Qualitatively, although all VRS were identifiable on both pre- and postmortem MRI, VRS appeared more distinct on T1w premortem scans compared to postmortem scans. This was confirmed in a quantitative analysis measuring VRS volume: Mean VRS volume was 12.6 µl (±SD: 10.2) in pre-mortem scans and 1.8 µl (±1.2) on postmortem scans (9 VRS, p = 0.006). In contrast, MS lesion volumes did not change significantly pre- versus post-mortem (premortem: 63.6 ± 47.7 µl, postmortem: 53.4 ± 48.1 µl, 8 MS lesions, p = 0.68) (Fig. 5a–c). Pre- and postmortem VRS did not correlate (r = 0.21, p = 0.57).

Histopathological validation of VRS
To assess the association of VRS with veins or arteries, VRS were localized on postmortem T1w MRI scans and subsequently correlated to their corresponding tissue substrate (Fig. 5d–f). In total, we assessed 20 VRS in MS cases and 8 VRS in control subjects (Supplementary Table S5). In the centrum semiovale, most VRS were associated with arterial vessels: out of 20 assessed VRS, 17 were associated with arteries (85%, Fig. 5g) and 3 with veins, all of them in the MS patients (Fig. 5h). In the basal ganglia, all VRS were associated with arteries (8 VRS, Supplementary Figure S4a). Of note, perimortem collapse of blood vessels can cause artificial widening of the perivascular space. Hence, we additionally identified the true perivascular compartment with a double staining for laminin α1 (labelling the parenchymal basement membrane) and collagen IV α1 (labelling the vascular basement membrane) (Fig. 5i and j).

Finally, we assessed the potential association of VRS with MS pathology features. Neither dilated nor non-dilated VRS were associated with adjacent demyelination (dilated VRS score: 0.75 [±SD: 0.71], non-dilated VRS score: 0.96 [±SD: 0.71]), perivascular cuffs (1.00 [±SD: 1.14], 0.81 [±SD: 1.01]), macrophage/microglial activation (2.00 [±SD: 2.14], 0.82 [±SD: 0.69]), or axonal damage (number of axons: 204 [±SD: 24], 211 [±SD: 78]) (Fig. 5k–p). There was no difference in AQP-4 staining between dilated and non-dilated VRS (Supplementary Figure S4b and S4c). Furthermore, VRS were not associated with perivascular amyloid deposition

ID, sex, age	Diagnosis	Cause of death	Post-mortem interval	MRI VRS burden	Number of retrieved tissue blocks	Pre- to post-mortem MRI interval
MS patients						
MS1, M, 60	PPMS	Brainstem stroke	9 h	High	14	16 months
MS2, F, 60	Progressive MS	Sepsis	7.5 h	Medium to high	5	N/A
MS3, F, 78	Progressive MS	Pneumonia	26 h	Medium	7	N/A
MS4, F, 57	SPMS	Unknown	89 h	High[a]	5	9 months
MS5, F, 78	Progressive MS	Unknown	12–15 h	Medium	2	N/A
MS6, F, 76	RRMS	Unknown	<24 h	High	9	8 months
Controls						
C1, M, 46	X-ALD	Sepsis	48 h	Low	4	N/A
C2, F, 71	Brain metastases (primary tumour unknown)	Unknown	<24 h	Medium	3	N/A
C3, M, 62	Subarachnoid bleeding	Pneumonia	<24 h	Medium	2	N/A

Brains from 6 multiple sclerosis (MS) patients and 3 control subjects were investigated for histopathological validation of (dilated) Virchow-Robin spaces (VRS). Abbreviations: MRI, magnetic resonance imaging; N/A, not available; PPMS, primary progressive multiple sclerosis; SPMS, secondary progressive multiple sclerosis; RRMS, relapsing-remitting multiple sclerosis; X-ALD, X-linked adrenoleukodystrophy. [a]No postmortem MRI available. The VRS burden was evaluated macroscopically on brain slabs.

Table 3: Post-mortem multiple sclerosis (MS) cohort.

(Supplementary Figure S4d and S4e). VRS were also not associated with perivascular fibrin deposition indicating blood-brain barrier (BBB) leakage (Supplementary Figure S4f and S4g). Interestingly, dilated VRS in the centrum semiovale were more commonly associated with signs of small vessel disease, such as splitting of the internal elastic lamina or vessel wall hyalinosis (Fig. 5q–s), compared to non-dilated VRS (Fig. 5t). This was confirmed in a quantitative analysis comparing the small vessel disease scores in dilated versus non-dilated VRS (dilated VRS: 3.86 [±SD: 1.34], non-dilated VRS: 2.21 [±SD: 0.89], p = 0.03). Such an association was not found in 3 control subjects without MS (8 VRS, dilated VRS: 2.44 [±SD: 1.44], non-dilated VRS: 2.02 [±SD: 1.01], p = 0.65).

Discussion
Main findings
The objective of this study was to investigate the potential association of nondilated and dilated VRS with clinical and imaging parameters in MS. Furthermore, we assessed the histopathological signature of VRS in a post-mortem cohort of 6 MS patients. In the MS cohorts, the count of dilated centrum semiovale VRS (diameter ≥ 2 mm), but not total VRS counts or volumes, was associated with increased T1 and T2 lesion volumes. VRS did not colocalize with T1 and T2 lesions at the anatomical level. Instead, they mostly corresponded to arteries and were not associated with common MS pathology features such as demyelination, axonal damage, or immune cell infiltration. However, intriguingly, the tissue signature of dilated VRS in the centrum semiovale corresponded to signs of arterial disease, despite the fact that focal demyelination in the MS white matter is a perivenular process.

Findings in the context of existing evidence
We have recently conducted a meta-analysis that substantiated the notion that MS patients carry a higher VRS burden compared to controls.[15] Findings from our current original study are in line with this notion. Additionally, in the current study, the count of dilated centrum semiovale VRS (diameter ≥ 2 mm), but not their volume or count, was associated with increased T1 and T2 lesion volume. Likewise, two other previous studies did not find an association of total VRS volume and/or count with T1 and/or T2 lesion burden.[14,16] However, these two studies did not assess dilated VRS. In contrast to the association with T1 and T2 lesion volumes, our analyses did not disclose an association between VRS measures and physical or cognitive disability in MS. It might be that our analyses were confounded by the relatively low level of physical and cognitive disability in our cohorts.

The association of VRS with neuroinflammatory pathology has been shown previously. Notably, a longitudinal study observed a VRS volume increase preceding the emergence of contrast-enhancing MS lesions[16] Thereupon, it has been speculated that the antecedent surge in VRS volume could represent a local accumulation of immune cells within the perivascular spaces. Focal perivascular space dilation has also been observed in a case series at the edges of active MS lesions at the initiation of inflammatory exacerbation[31] However, in our longitudinal cohort, we did not find an association between VRS outcomes and gadolinium-enhancing, T1, or T2 lesions. Furthermore, T1 and T2 lesions did not spatially cluster with VRS. Also, the absence of common MS pathology features adjacent to VRS, including the lack of perivascular cuffing, renders their direct association with neuroinflammatory tissue pathology unlikely.

Clinical MRI at conventional field strengths cannot easily discriminate perforating arterioles and venules.
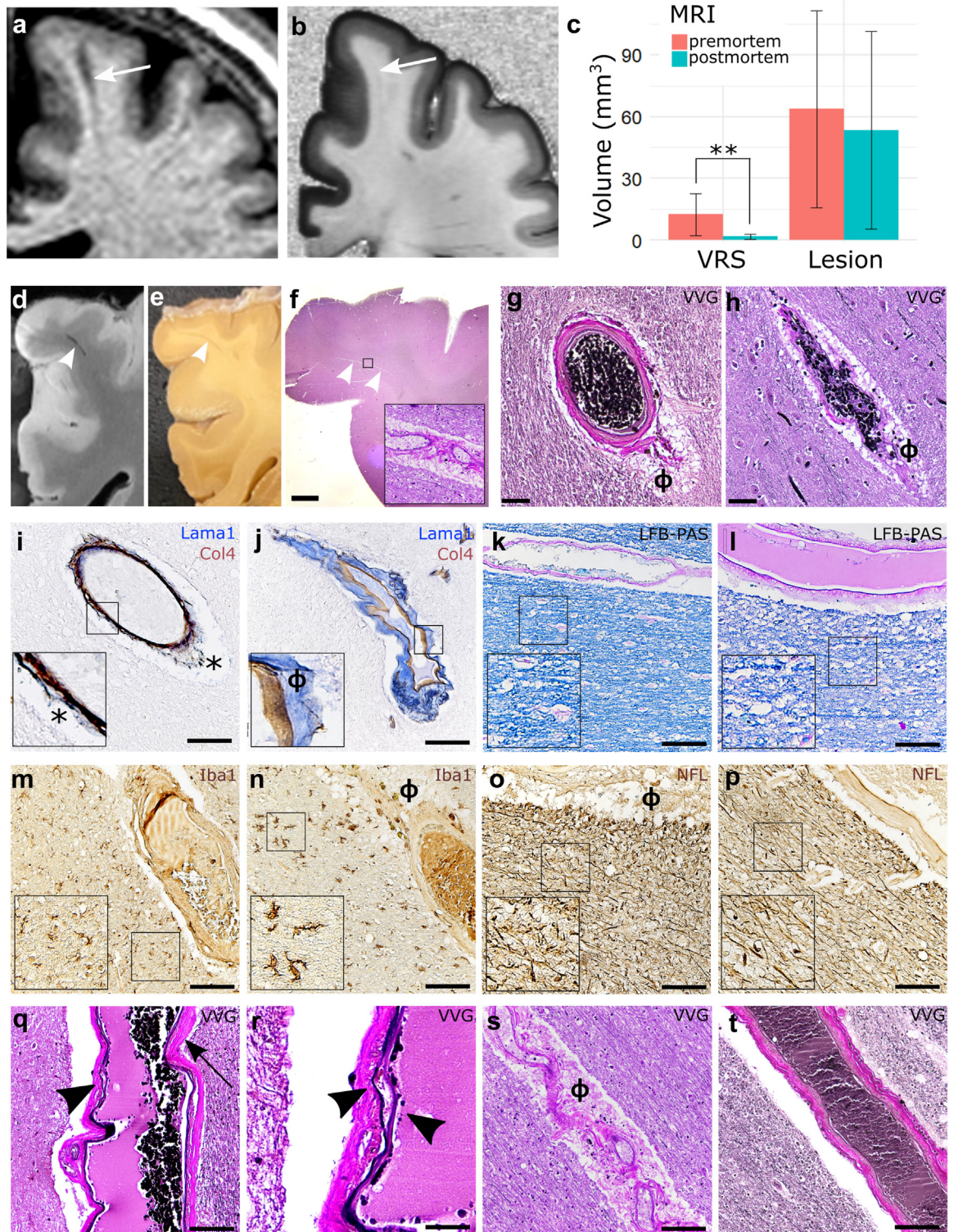
Fig. 5: Histopathological validation of dilated and non-dilated VRS. (a–c): Dynamic changes of pre- (a) versus post-mortem VRS (b): VRS show a substantial drop in volume from pre- to post-mortem MRI (quantification: (c)). (d–f): VRS, as identified on postmortem T1w MRI scans (d), were correlated to corresponding brain tissue blocks I and paraffin tissue slices ((f), inlet with 200× magnification). VRS corresponded mostly to arteries ((g), ϕ = perivascular space) and to a lesser extent veins (h). (i and j): The perivascular compartments were identified with double

Thus, it is currently under debate whether VRS surround arterial or venous vessels or both.[2,7] A small imaging study employing structural T2w MRI scans in conjunction with angiographies at ultra-high static magnetic field strengths found that VRS correspond to arterial vessels.[32] Our MRI-histology correlation of VRS corroborates this observation by providing histological evidence that VRS in the centrum semiovale and basal ganglia mostly correspond to arteries. Because perivascular cuffing in MS is commonly observed surrounding venules,[33] this notion further argues against the hypothesis that dilation of VRS corresponds to perivascular cuffing.[16]

An increase of VRS has been consistently associated with ageing,[8] which is also confirmed by our data from MS patients, though naturally chronologically confounded by the disease duration. Based on this association with ageing, it has also been speculated that VRS represent a perivascular *ex vacuo* atrophy.[3] In MS, a study employing ultra-high-field MRI found that higher VRS counts were associated with lower brain parenchymal fraction.[13] Our study does not support this observation: dilation of VRS was not explained by higher degrees of brain volume loss in our MS cohort. Furthermore, we did not find myelin pallor or apparent loss of axonal density as signs of Wallerian degeneration adjacent to VRS.[34] Nevertheless, more widespread neurodegeneration and/or volume loss of extra-neuronal tissue components cannot easily be ruled out by histopathological analysis.

VRS have been associated with small vessel disease[6] and cardiovascular risk factors such as hypertension.[35] Interestingly, in cerebral amyloid angiopathy, the degree of VRS dilation was associated with more pronounced accumulation of Aβ in upstream juxtacortical vessel walls.[36] While we did not observe vascular Aβ deposition in VRS in our histopathological analysis, we did find more distinct signs of arterial pathology in dilated versus nondilated VRS in MS compared to non-MS controls. This is in line with observations from a large postmortem study in MS patients reporting higher cerebral small vessel disease features such as periarteriolar space dilation in MS patients.[37] Interestingly, vascular comorbidities have been associated with worse cognitive function[38] and lower brain volumes in MS[39] (reviewed in[40]). This is in line with our observations that dilated VRS—corresponding to arteries with vascular disease—are associated with higher T1 and T2 lesion volumes. This opens the question about the pathological cascade of these events, i.e., does vascular disease precipitate neuroinflammation or does chronic neuroinflammation and its downstream effects cause vascular disease? A large genome-wide association study did not provide evidence to suggest a shared genetic mechanism of ischemic white matter damage and MS.[41] Furthermore, the association between dilated VRS and lesion volumes was statistically independent from general vascular risk factors in our study, which may indicate a more direct causal link between VRS and MS pathology. In contrast, it has been shown in a neuroinflammatory marmoset model that intralesional veins can show vascular remodeling with perivascular collagen deposition already during early lesion emergence.[42] It can be speculated that similar mechanisms might contribute to arterial pathology in chronic and widespread neuroinflammation like in MS.

There is insufficient understanding of how VRS become dilated[5]: it has been hypothesized that perivascular fibrosis, *ex vacuo* atrophy of adjacent brain tissue, or alterations of arterial wall permeability might cause dilation. Our data add the notion that arterial disease could also cause VRS dilation. In addition, the local widening of the perivascular spaces in the juxtacortical white matter, e.g., in the centrum semiovale, could indicate impaired interstitial or cerebrospinal fluid drainage[43] and/or excess fluid leakage from the vasculature.[44] In our pre- and postmortem MRI comparison, the numbers of VRS remained similar, in line with findings from a recent MRI-postmortem study.[45] However, we observed a strong decrease in VRS volumes upon death. It is unclear to what extent this comes from a drop of blood or CSF pressure or both, but this observation could allude toward increased local CSF pressure. To further test this hypothesis, sensitive imaging methods are warranted to visualize BBB pathology and/or perivascular fluid drainage in proximity to VRS, such as dynamic contrast enhanced MRI[46] or CSF tracer studies.[47]

Limitations
Our study has some limitations: (1) Our longitudinal cohort only included 24 patients with longitudinal scans (followed-up for 31.5 patient years). Although this is one of the largest longitudinal cohorts of VRS in MS to date,

staining for laminin α1 (labelling the parenchymal basement membrane, blue) and collagen IV α1 (labelling the vascular basement membrane, brown) (j) which was in contrast to artifacts caused by perimortem vascular collapse (asterisk, (i); inlets with 200× magnification). (k–p): Neither dilated (k, m, o, q, s) nor nondilated VRS (l, n, p, r, t) were associated with demyelination ((k and l), LFB-PAS), activation of microglia/macrophages ((m and n), Iba1), or axonal damage (o and p), neurofilament [NFL]; insets with 200× magnification). (q–t): Dilated VRS of the arterial tree were more commonly associated with signs of small vessel disease, such as splitting of the internal elastic lamina (arrowhead in (q), 200× magnification, higher magnification in (r), vessel wall hyalinosis (arrow in (q)), or vascular tortuosity (s) compared to nondilated VRS (t). Scale bars = 50 μm, except in f = 1 mm and r = 10 μm. *Abbreviations:* ϕ, perivascular space; LFB-PAS, Luxol Fast Blue periodic acid-Schiff; MRI, magnetic resonance imaging; VVG, Verhoeff van Gieson; VRS, Virchow-Robin space.

the cohort size is relatively small compared with those investigated for other MRI outcomes. Development of automated tools for VRS identification and segmentation could facilitate larger studies with longer follow-up. (2) Our clinical cohort comprises a relatively large proportion of patients with highly effective DMT such as B cell-depleting therapies, which frequently are used among Swedish MS patients.[48] This warrants a cautious interpretation of findings in relation to earlier studies such as the one by Wuerfel and colleagues DMTs.[16] (3) In our post-mortem cohort, 5 of 6 patients had a progressive clinical MS phenotype, contrasting with the mostly relapsing clinical phenotype of the *in vivo* cohort. This predominance of more chronic disease could have biased our analysis, i.e., findings might not be generalizable to MS patients with early and highly active disease.

Conclusions

In MS, higher numbers of centrum semiovale dilated VRS were associated with greater T1 and T2 lesion volumes. Correlative histopathology showed that these VRS mostly corresponded to arteries displaying signs of vascular disease but no MS pathology hallmarks. Collectively, these data questions the hypothesis that the dilation of perivascular spaces represents a surge of immune cells prior to a neuroinflammatory outbreak. Instead, our data suggest the possibility of an association of MS with arterial disease. To corroborate these findings, future studies should longitudinally assess VRS dynamics and their association with markers of small vessel disease.

References
1 Wardlaw JM, Smith EE, Biessels GJ, et al. Neuroimaging standards for research into small vessel disease and its contribution to ageing and neurodegeneration. *Lancet Neurol*. 2013;12(8):822–838.
2 Barisano G, Lynch KM, Sibilia F, et al. Imaging perivascular space structure and function using brain MRI. *Neuroimage*. 2022;257:119329.
3 Ineichen BV, Okar SV, Proulx ST, Engelhardt B, Lassmann H, Reich DS. Perivascular spaces and their role in neuroinflammation. *Neuron*. 2022;110(21):3566–3581.
4 Kwee RM, Kwee TC. Virchow-Robin spaces at MR imaging. *Radiographics*. 2007;27(4):1071–1086.
5 Rudie JD, Rauschecker AM, Nabavizadeh SA, Mohan S. Neuroimaging of dilated perivascular spaces: from benign and pathologic causes to mimics. *J Neuroimaging*. 2018;28(2):139–149.
6 Debette S, Schilling S, Duperron MG, Larsson SC, Markus HS. Clinical significance of magnetic resonance imaging markers of vascular brain injury: a systematic review and meta-analysis. *JAMA Neurol*. 2019;76(1):81–94.
7 Wardlaw JM, Benveniste H, Nedergaard M, et al. Perivascular spaces in the brain: anatomy, physiology and pathology. *Nat Rev Neurol*. 2020;16(3):137–153.
8 Francis F, Ballerini L, Wardlaw JM. Perivascular spaces and their associations with risk factors, clinical disorders and neuroimaging features: a systematic review and meta-analysis. *Int J Stroke*. 2019;14(4):359–371, 1747493019830321.
9 Aribisala BS, Wiseman S, Morris Z, et al. Circulating inflammatory markers are associated with magnetic resonance imaging-visible perivascular spaces but not directly with white matter hyperintensities. *Stroke*. 2014;45(2):605–607.
10 Doubal FN, MacLullich AM, Ferguson KJ, Dennis MS, Wardlaw JM. Enlarged perivascular spaces on MRI are a feature of cerebral small vessel disease. *Stroke*. 2010;41(3):450–454.
11 Lau K-K, Li L, Lovelock CE, et al. Clinical correlates, ethnic differences, and prognostic implications of perivascular spaces in transient ischemic attack and ischemic stroke. *Stroke*. 2017;48(6):1470–1477.
12 Ramirez J, Berezuk C, McNeely AA, Gao F, McLaurin J, Black SE. Imaging the perivascular space as a potential biomarker of neurovascular and neurodegenerative diseases. *Cell Mol Neurobiol*. 2016;36(2):289–299.
13 Kilsdonk ID, Steenwijk MD, Pouwels PJ, et al. Perivascular spaces in MS patients at 7 Tesla MRI: a marker of neurodegeneration? *Mult Scler*. 2015;21(2):155–162.
14 Cavallari M, Egorova S, Healy BC, et al. Evaluating the association between enlarged perivascular spaces and disease worsening in multiple sclerosis. *J Neuroimaging*. 2018;28(3):273–277.
15 Granberg T, Moridi T, Brand JS, et al. Enlarged perivascular spaces in multiple sclerosis on magnetic resonance imaging: a systematic review and meta-analysis. *J Neurol*. 2020;267(11):3199–3212.
16 Wuerfel J, Haertle M, Waiczies H, et al. Perivascular spaces–MRI marker of inflammatory activity in the brain? *Brain*. 2008;131(Pt 9):2332–2340.
17 Etemadifar M, Hekmatnia A, Tayari N, et al. Features of Virchow-Robin spaces in newly diagnosed multiple sclerosis patients. *Eur J Radiol*. 2011;80(2):e104–e108.
18 Kurtzke JF. Rating neurologic impairment in multiple sclerosis: an expanded disability status scale (EDSS). *Neurology*. 1983;33(11):1444–1452.
19 Smith A. *Symbol digit modalities test*. Los Angeles, CA: Western Psychological Services; 1982.
20 Lezak M, Howieson D, Bigler E, Tranel D. *Neuropsychological assessment*. 5 2012.
21 Jenkinson M, Beckmann CF, Behrens TE, Woolrich MW, Smith SM. FSL. *Neuroimage*. 2012;62(2):782–790.
22 Fischl B. FreeSurfer. *Neuroimage*. 2012;62(2):774–781.
23 Rudick RA, Fisher E, Lee JC, Simon J, Jacobs L. Use of the brain parenchymal fraction to measure whole brain atrophy in relapsing-remitting MS. Multiple Sclerosis Collaborative Research Group. *Neurology*. 1999;53(8):1698–1704.
24 Schmidt P, Mühlau M, Gaser C, Wink L. *LST: a lesion segmentation tool for SPM*. Acesso em. 2013.

25 ITK-SNAP: an interactive tool for semi-automatic segmentation of multi-modality biomedical images. In: Yushkevich PA, Gao Y, Gerig G, eds. *2016 38th Annual international conference of the IEEE engineering in medicine and biology society (EMBC)*. IEEE; 2016.

26 Favaretto A, Lazzarotto A, Riccardi A, et al. Enlarged Virchow Robin spaces associate with cognitive decline in multiple sclerosis. *PLoS One*. 2017;12(10):e0185626.

27 Absinta M, Nair G, Filippi M, et al. Postmortem magnetic resonance imaging to guide the pathologic cut: individualized, 3-dimensionally printed cutting boxes for fixed brains. *J Neuropathol Exp Neurol*. 2014;73(8):780–788.

28 Luciano NJ, Sati P, Nair G, et al. Utilizing 3D printing technology to merge MRI with histology: a protocol for brain sectioning. *J Vis Exp*. 2016;(118):54780.

29 Grinberg LT, Thal DR. Vascular pathology in the aged human brain. *Acta Neuropathol*. 2010;119(3):277–290.

30 Fischl B, Salat DH, Busa E, et al. Whole brain segmentation: automated labeling of neuroanatomical structures in the human brain. *Neuron*. 2002;33(3):341–355.

31 Ge Y, Law M, Herbert J, Grossman RI. Prominent perivenular spaces in multiple sclerosis as a sign of perivascular inflammation in primary demyelination. *Am J Neuroradiol*. 2005;26(9):2316–2319.

32 Bouvy WH, Biessels GJ, Kuijf HJ, Kappelle LJ, Luijten PR, Zwanenburg JJ. Visualization of perivascular spaces and perforating arteries with 7 T magnetic resonance imaging. *Invest Radiol*. 2014;49(5):307–313.

33 Sati P, Oh J, Constable RT, et al. The central vein sign and its clinical evaluation for the diagnosis of multiple sclerosis: a consensus statement from the North American Imaging in Multiple Sclerosis Cooperative. *Nat Rev Neurol*. 2016;12(12):714–722.

34 Dal-Bianco A, Grabner G, Kronnerwetter C, et al. Long-term evolution of multiple sclerosis iron rim lesions in 7 T MRI. *Brain*. 2021;144(3):833–847.

35 Ballerini L, Lovreglio R, Valdes Hernandez MDC, et al. Perivascular spaces segmentation in brain MRI using optimal 3D filtering. *Sci Rep*. 2018;8(1):2132.

36 Van Veluw SJ, Biessels GJ, Bouvy WH, et al. Cerebral amyloid angiopathy severity is linked to dilation of juxtacortical perivascular spaces. *J Cerebr Blood Flow Metabol*. 2016;36(3):576–580.

37 Geraldes R, Esiri MM, Perera R, et al. Vascular disease and multiple sclerosis: a post-mortem study exploring their relationships. *Brain*. 2020;143(10):2998–3012.

38 Marrie RA, Patel R, Figley CR, et al. Effects of vascular comorbidity on cognition in multiple sclerosis are partially mediated by changes in brain structure. *Front Neurol*. 2022;13:910014.

39 Fitzgerald KC, Damian A, Conway D, Mowry EM. Vascular comorbidity is associated with lower brain volumes and lower neuroperformance in a large multiple sclerosis cohort. *Mult Scler J*. 2021;27(12):1914–1923.

40 Geraldes R, Esiri MM, DeLuca GC, Palace J. Age-related small vessel disease: a potential contributor to neurodegeneration in multiple sclerosis. *Brain Pathol*. 2017;27(6):707–722.

41 Brown RB, Traylor M, Burgess S, Sawcer S, Markus HS. Do cerebral small vessel disease and multiple sclerosis share common mechanisms of white matter injury? A genetic study. *Stroke*. 2019;50(8):1968–1972.

42 Absinta M, Nair G, Monaco MCG, et al. The "central vein sign" in inflammatory demyelination: the role of fibrillar collagen type I. *Ann Neurol*. 2019;85(6):934–942.

43 Bakker EN, Bacskai BJ, Arbel-Ornath M, et al. Lymphatic clearance of the brain: perivascular, paravascular and significance for neurodegenerative diseases. *Cell Mol Neurobiol*. 2016;36(2):181–194.

44 Nation DA, Sweeney MD, Montagne A, et al. Blood–brain barrier breakdown is an early biomarker of human cognitive dysfunction. *Nat Med*. 2019;25(2):270–276.

45 Haider L, Hametner S, Endmayr V, et al. Post-mortem correlates of Virchow-Robin spaces detected on *in vivo* MRI. *J Cerebr Blood Flow Metabol*. 2016;36(11):1628–1638.

46 Quarles CC, Bell LC, Stokes AM. Imaging vascular and hemodynamic features of the brain using dynamic susceptibility contrast and dynamic contrast enhanced MRI. *Neuroimage*. 2019;187:32–55.

47 Ringstad G, Valnes LM, Dale AM, et al. Brain-wide glymphatic enhancement and clearance in humans assessed with MRI. *JCI Insight*. 2018;3(13):e121537.

48 Ineichen BV, Moridi T, Granberg T, Piehl F. Rituximab treatment for multiple sclerosis. *Mult Scler*. 2019;26(2):137–152, 1352458519858604.